International Journal of Innovative Technologies
WWW.IJITECH.ORG
ISSN 2321-8665
Vol.03,Issue.02,
June-2015,
Pages:0077-0082

Evaluation of Ancient Documents and Images by using Phase Based Binarization

K. SRUJANA[1], D. C. VINOD R KUMAR[2]
[1]PG Scholar, Dept of ECE, Global College of Engineering & Technology, Kadapa, YSR (Dt), AP, India.
[2]Assistant Professor, Dept. of ECE, Global College of Engineering & Technology, Kadapa, YSR (Dt), AP, India.

Abstract: Segmentation of text from badly degraded document images are a very challenging task due to the high inters/intravariation between the document background and the foreground text of different document images. These features are the maximum moment of phase congruency covariance, a locally weighted mean phase angle, and a phase preserved denoised image. The proposed model consists of three standard steps: 1) preprocessing; 2) main binarization; and 3) postprocessing. In the preprocessing and main binarization steps, the features used are mainly phase derived, while in the postprocessing step, specialized adaptive Gaussian and median filters are considered. One of the outputs of the binarization step, which shows high recall performance, is used in a proposed postprocessing method to improve the performance of other binarization methodologies. Finally, we develop a ground truth generation tool, called PhaseGT, to simplify and speed up the ground truth generation process for ancient document images. The comprehensive experimental results on the DIBCO'09, H-DIBCO'10, DIBCO'11, H-DIBCO'12, DIBCO'13, PHIBD'12, and BICKLEY DIARY data sets show the robustness of the proposed binarization method on various types of degradation and document images. Experiments on the Bickley diary dataset that consists of several challenging bad quality document images also show the superior performance of our proposed method, compared with other techniques.

Keywords: Historical Document Binarization, Phase-Derived Features, Ground Truthing, Document Enhancement.

I. INTRODUCTION

Document Image Binarization is performed in the preprocessing stage for document analysis and it aims to segment the foreground text from the document background. A fast and accurate document image binarization technique is important for the ensuing document image processing tasks such as optical character recognition (OCR). Though document image binarization has been studied for many years, the thresholding of degraded document images is still an unsolved problem due to the high inter/intravariation between the text stroke and the document background across different document images. The enormous quantity of digital information fashioned requires automatic processing, enhancement, and acknowledgment. A key step in all document image processing workflows is binarization, but this is not a very sophisticated process, which is unfortunate, as its performance has a significant influence on the quality of OCR results. Many investigate studies have been approved out to solve the problems that arise in the binarization of old document images characterized by many types of degradation, including faded ink, bleed-through, show-through, uneven illumination, variations in image contrast, and weakening of the cellulose structure [1], [20]. There are also differences in patterns of hand-written and machine-printed documents, which add to the difficulties associated with the binarization of old document images.

Fig.1. Sample document images selected from the DIBCO'09 [21], H-DIBCO'10 [22], and DIBCO'11 datasets [23].

To the most excellent of our acquaintance, none of the proposed methods can deal with all types of documents and degradation. For more details, see the Related Work section. Fig. 1 shows some of the degraded document images used in this paper. In this paper, a robust phase-based binarization method is proposed for the binarization and enhancement of historical documents and manuscripts. The proposed binarization method is stable and robust to various types of degradation and to different datasets, thanks to its purpose-designed steps, and we provide comprehensive experimental results to demonstrate this robustness. The method

outperforms most of the algorithms entered in the DIBCO'09 [21], H-DIBCO'10 [22], DIBCO'11 [23], H-DIBCO'12 [32], DIBCO'13 [33] and PHIBC'12 [34] competitions, based on various evaluation measures, including the F-measure, NRM, PSNR, DRD, and MPM. The second contribution of this paper is the proposal of a fast, semi-automatic tool for ground truth (GT) creation using robust phase-based feature maps. GT generation for degraded document images is a difficult and time-consuming task, even for experts; however, benchmark datasets are required for the evaluation of binarization methods.

II. PHASE-DERIVED FEATURES

In this paper we used three phase-derived feature maps of the input document image. The details are provided below.

A. Phase Congruency-Based Feature Maps

In this section, two phase congruency-based feature maps extracted from input images are discussed. These feature maps are based on the Kovesi's phase congruency model. Another approach to the phase-based processing of images could be the monogenic scale-space method of [43]. However, based on our experiments, Kovesi's method worked better within our proposed binarization method. In phase congruency, the pixels of interest are at those points where the phase of the Fourier components is at its maximal [26], [44]. Let M_n^e and M_ρ^o denote the even symmetric and odd symmetric log-Gabor wavelets at a scale ρ, which are known in the literature as quadratic pairs [45].

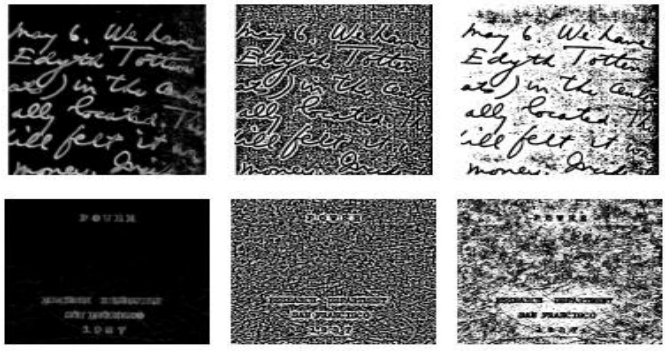

(a) (b) (c)

Fig. 2. Two examples of IM, IL, and ID maps.

The pixels of IL take values between $-\pi/2$ (a dark line) and $+\pi/2$ (a bright line). It is worth mentioning that if we use the same definition of local phase as that of equation (2) for IL, the IL values would be in the interval of $[0, \pi]$. There are several parameters to be considered in the calculation of IM and IL. Unfortunately, these parameters are set based on experiments in the literature.

B. Phase Preserving Denoising

An image denoising method proposed by Kovesi [24] is used in this paper, which is based on the supposition that phase information is the most significant trait of images. This method also attempts to preserve the perceptually important phase information in the signal. It uses non-orthogonal, complex valued log-Gabor wavelets, which extract the local phase and amplitude information at each point in the image. The denoising process consists of determining a noise threshold at each scale and shrinking the magnitudes of the filter response vector appropriately, while leaving the phase unchanged. Automatic estimation of these noise thresholds, using the statistics of the smallest filter scale response, is the most important part of denoising.

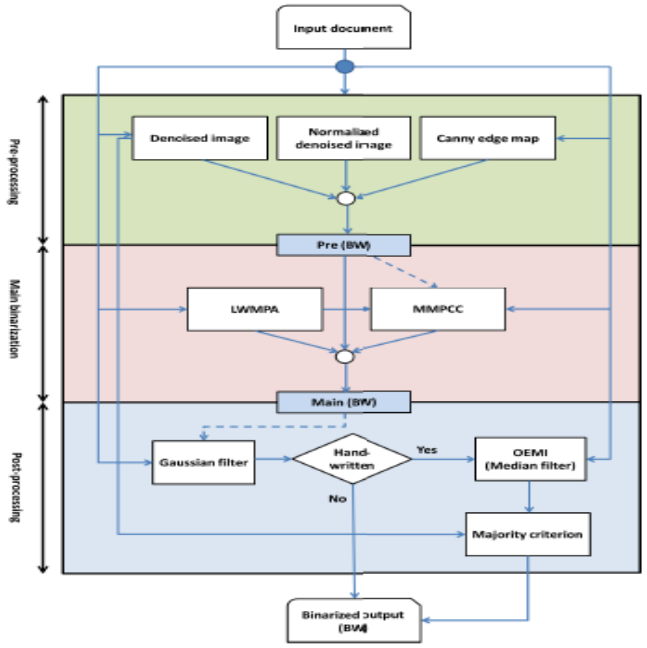

Fig. 3. Flowchart of the proposed binarization method.

These statistics are used to estimate the distribution of the noise amplitude, because they give the strongest noise response. Then, the noise amplitude distribution of other filter scales can be estimated proportionally. Supposing that μ_R denotes the mean and σ^2_R denotes the variance of the Rayleigh distribution, the noise shrinkage threshold can be computed using equation (14). For each orientation, noise responses from the smallest scale filter pair are estimated and a noise threshold is obtained. This noise response distribution is used to estimate the noise amplitude distribution of other filter scales using some constant. Finally, based on the noise thresholds obtained, the magnitudes of the filter response vectors shrink appropriately, and they do so by soft thresholding, while leaving the phase unchanged. Fig. 2 shows two examples of IM, IL, and ID maps, where ID denotes the denoised image. The solid lines show the binary output of this step, the dashed line shows that the binary output is also used to tune parameters of a step, and the white circles denote the pixel-wise AND operator.

III. BINARIZATION MODEL

The final binarized output image is obtained by processing the input image in three steps: preprocessing, main binarization, and postprocessing as shown in Fig.3. The binarization model is an extended version of the one proposed in our previous.

A. Preprocessing

In this we use a denoised image instead of the original image to obtain a binarized image in rough form. The image denoising method discussed in section III is applied to preprocess the binarization output. A number of parameters impact the quality of the denoised output image (ID), the key

ones being the noise standard deviation threshold to be rejected (k), and the number of filter scales (N_ρ) and the number of orientations (N_r) to be used. The N_ρ parameter controls the extent to which low frequencies are covered. The higher N_ρ is, the lower the frequencies, which means that the recall value remains optimal or near optimal. Based on our experiments, $N_\rho = 5$ is the appropriate choice in this case. Therefore, to preserve all the foreground pixels, we set the parameters in the experiments as follows: $k = 1$, $N_\rho = 5$ and $N_r = 3$. We used Otsu's method on the normalized denoised image, where normalized denoised image is obtained by applying a linear image transform on the denoised image. This approach can also remove noisy and degraded parts of images, because the denoising method attempts to shrink the amplitude information of the noise component.

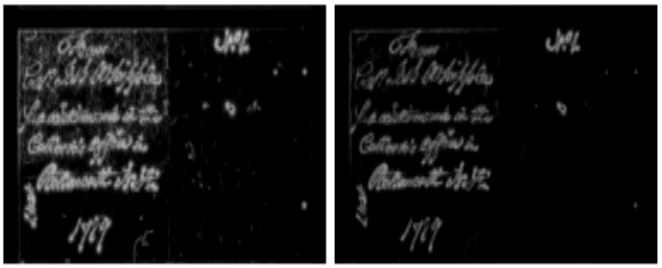

(a) (b)

Fig. 4. The output of IM with a) fixed noise parameter [18], [19], an b) adaptive noise parameter estimation.

B. Main Binarization

The next step is the main binarization, which is based on phase congruency features: i) the maximum moment of phase congruency covariance (IM); and ii) the locally weighted mean phase angle (IL).

IM: IM is used to divide the background from potential foreground parts. This step performs very well, even in badly degraded documents, where it can reject a majority of badly degraded background pixels by means of a noise modeling method. To achieve this, we set the number of two-dimensional log-Gabor filter scales ρ to 2, and use 10 orientations of two-dimensional log-Gabor filters r. Fig. 4 shows the output of IM with and without using equation (20) to compute k. Note the different values used for setting the phase congruency feature and denoised image parameters. Fig. 5 shows an example of how we use IM to remove a majority of the background pixels.

IL: The parameters used to obtain the IM and IL maps, IL produces some classification errors on the inner pixels of large foreground objects. Using more filter scales would solve this problem, but reduce the performance of IL on the strokes. Also, IL impacts the quality of the IM edge map, and of course requires more computational time. Nevertheless, the results of using Otsu's method to binarize the large foreground objects are of interest. Consequently, we used the IOtsu, bw image to overcome the problem.

C. Postprocessing

In this step, we apply enhancement processes. First, a bleed through removal process is applied. Then, a Gaussian filter is used to further enhance the binarization output and to separate background from foreground, and an exclusion process is applied, based on a median filter and IM maps, to remove background noise and objects. Finally, a further enhancement process is applied to the denoised image. The individual steps are as follows.

(a) (b) (c) (d) (e) (f)

Fig. 5. A degraded document image and its binarized image using phase congruency. a) Original degraded document image. b) Edge image obtained by phase congruency (IM). c) Filled image of IM. d) Binarization of (c) using Otsu's method. e) Denoised image and f) The result of main binarization.

Global Bleed-Through Exclusion: In this paper, bleed-through is categorized in two classes: i) local bleed through and ii) global bleed-through. Local bleed-through involves pixels located under or near foreground pixels, while global bleed-through involves pixels located far away the foreground text. At this stage, we investigate the possibility of the existence of global bleed-through. If it does exist, the parameters of the Canny edge detector are chosen to ensure that the output edge map contains only the edges of text regions which we expect to be located in a specific part, or parts, of the image.

Adaptive Gaussian Filter: In this section, we take a similar approach to the one used in [47], except that a Gaussian smoothing filter is used to obtain a local weighted mean as the reference value for setting the threshold for each pixel as shown in Fig.6. We use a rotationally symmetric Gaussian low-pass filter (G) of size S with σ value, estimated based on average stroke-width, where σ is the standard deviation. This is a modification of the fixed S value used in [19]. The value for S is the most important parameter in this approach. A pixel is set to 0 (dark) if the value of that pixel in the input image is less than 95% of the corresponding threshold value T (x, y), and it is set to 1 (white) otherwise. We increased the value from 85% [47] to 95%, in order to obtain a near optimal recall value.

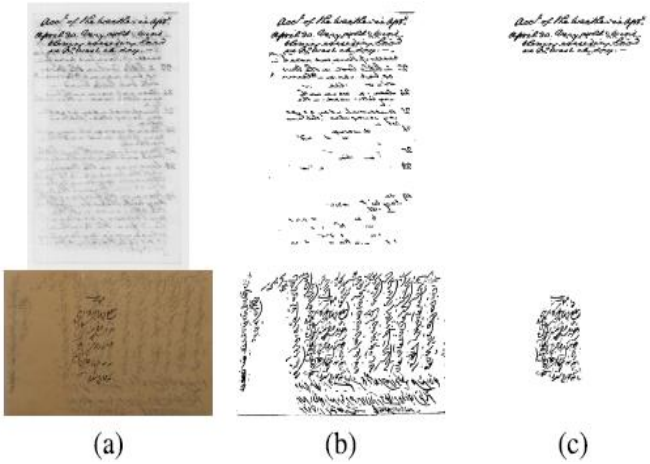

Fig. 6. Effect of using the proposed global bleed-through exclusion is shown in column (c). The left image (b) is the binarized image before the global bleed-through exclusion step has been applied.

Document Type Detection: At this step, we need to determine the type of input document we are dealing with. We propose to apply the enhancement processes that are after this step to the handwritten documents only, and not to machine printed documents. The method we propose for detecting the type of document is straightforward and fast. We use the standard deviation of the orientation image that was produced during calculation of the phase congruency features. This image takes positive anticlockwise values between 0 and 180. A value of 90 corresponds to a horizontal edge, and a value of 0 indicates a vertical edge. By considering the foreground

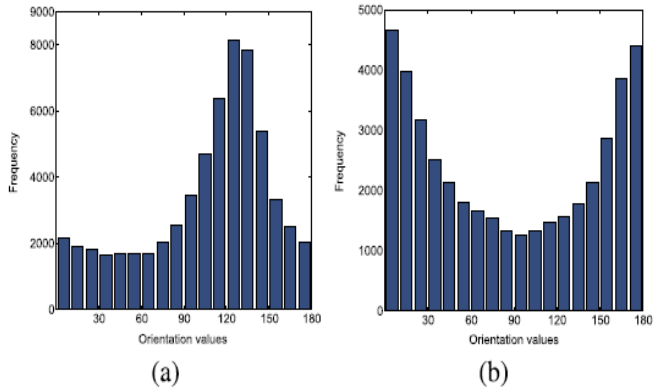

Fig. 7. Histogram of orientations of a handwritten document (a) and a machine-printed document (b).

pixels of the output binary image obtained so far, This approach works well for almost all the images we tested, including 21 machine-printed images and 60 handwritten document images, and only one classification error was found. It can be seen from the Fig.7 that the histogram of orientations of a handwritten document follows a U-shape behavior.

Object Exclusion Map Image (IOEM): We construct an object exclusion map image (IOEM) based on a combination of a median filter and a binary map of IM (see Algorithm 1). Any object without a reference in this binary map will be removed from the final binarization results. This approach can remove noise, local bleed-through, and interfering patterns.

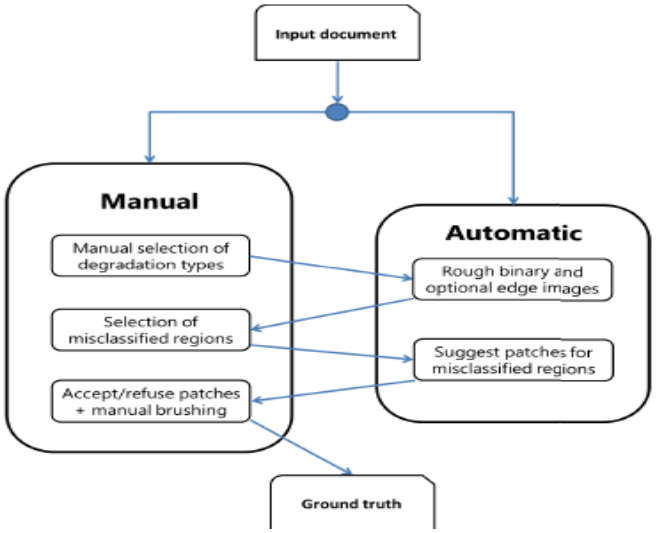

Fig.8. Flowchart of the proposed ground truthing tool (PhaseGT).

Majority Criterion: We propose a majority criterion based on a denoised image, ID. A majority criterion supposes that early binarization steps provide an optimal or near optimal recall value. Then, based on the fact that a foreground pixel should have a lower value than its adjacent background pixels, exclusion over the foreground pixels is performed.

IV. PHASEGT: AN EFFICIENT GROUND TRUTHING TOOL

We introduce a ground truthing application, called Phase GT, in this paper, and use it to generate ground truth images. Phase GT is mainly based on phase congruency features and a phase-denoised image. Fig. 8 shows how PhaseGT produces ground truth images in three steps:

- The user provides a priori information about the input document image. This information includes the type of image, e.g. machine-printed, handwritten, or a combination of the two. The user is then asked to choose degradation types from a list. If this is not possible, PhaseGT works in automatic mode to generate this intermediate output.
- PhaseGT preprocesses the input image and generates an intermediate ground truth binary image. The objective in this step is to save human interaction time.
- The user makes final modifications to the intermediate ground truth image. He can, for example, change pixels using brushing tools. He can also select a portion of the intermediate binary image that contains binarization errors, and choose from a number of replacement options offered by PhaseGT. This can save the user time by avoiding the need for manual corrections. Also, an optional edge map is provided by PhaseGT to help users choose the real edges of texts.

V. RESULTS AND DISCUSSION

The proposed binarization method is evaluated on a number of datasets. The following datasets were used: DIBCO'09 [21], H-DIBCO'10 [22], DIBCO'11 [23], H-DIBCO'12 [32], DIBCO'13 [33], PHIBD'12 [38], and

BICKLEY DIARY [53]. These datasets provide a collection of images that have suffered different types of degradation, and which give enough information and are sufficiently challenging in terms of evaluation setup to enable a meaningful examination of various algorithms. First, we compare the subjective and objective performance of the proposed method with that of leading binarization methods in the literature. Then, we compared our proposed binarization method with state-of-the-art algorithms and the top ranking algorithm in each competition.

A. Subjective Evaluation

In this section, we compare outputs of the proposed method with those of top-placing methods in each contest, whenever possible. Our proposed method performs a smooth binarization of the document images, thanks to the use of phase congruency measures and a denoised image. In Fig. 9, we compare the proposed method with three top-placing algorithms in DIBCO'11 [23], the winning algorithm in DIBCO'09 [21], and the method proposed in [10].

B. Objective Evaluation

We used the well-known measures F-measure (FM), pseudo F-measure (p-FM), PSNR, distance reciprocal distortion (DRD) metric [54], the misclassification penalty metric (MPM), the negative rate metric (NRM) to evaluate various

TABLE I: Comparison of the Performance of the Proposed Method and the Others against Dibco'09 Dataset

Algorithm	FM±std	FM*	PSNR	NRM	MPM
Proposed	92.52±2.34	**92.58**	19.00	**3.39**	0.54
Proposed (upper bound)	93.36±1.93	93.39	19.55	3.52	0.25
BE [9]	91.13±4.80	91.23	18.65	4.30	0.54
LMM [10]	91.06±2.93	91.18	18.50	6.54	0.45
Ms Gb Sauvola [1]	89.26±6.07	89.64	17.76	3.78	1.18
Sauvola Ms_{kx} [40]	76.85±20.27	80.14	14.52	4.71	8.95
AdOstu [3]	91.55±3.69	91.61	18.80	5.29	0.65
PC [19]	88.43±4.35	88.62	17.03	4.36	1.06
LMM+ [2]	**93.5**	-	**19.65**	3.74	**0.43**
1^{st} rank of contest	91.13±4.80	91.23	18.65	4.30	0.54
Best results of contest	91.13±4.80	91.23	18.66	4.18	0.52

algorithms [21]–[23]. The source code of the evaluation measures used in this paper is available in [55]. The results of the proposed method are compared with state-of-the-art binarization methods. Tables I-IV show the evaluation results obtained by the proposed method and state-of-the-art binarization algorithms for the DIBCO'09 [21], H-DIBDO'10 [22], DIBCO'11 [23], and BICKLEY DIARY [53] datasets respectively. PHIBD'12 is a dataset of historical Persian images consisting of 15 degraded document images.

The results show that the proposed method achieved, on average, a 5% improvement over our earlier results [19]. It can be seen from these experimental results that other binarization methods produce different results for different datasets, whereas there is little difference between the results we obtained using the proposed method on different datasets, which shows the robustness of our method. The upper bound performances of the proposed method when parameters of the proposed binarization method have been tuned are listed in Tables I-VII. Also, the best value from each contest is provided in the last row of Tables I-VI. For having a fair comparison in Table VI, the best results for each measure is not highlighted because GTs of PHIBD'12 are generated using phase-congruency features and this might boosted the performance of the proposed method. In this paper, the standard deviation of the numerical results is considered to measure the reliability of the various methods we compared. The results in Tables I-V show that the proposed algorithm shows the lowest variation among the methods in terms of FM variations.

TABLE II: Comparison Of The Performance Of The Proposed Method And The Others Against H-Dibco'10 Dataset

Algorithm	FM±std	FM*	p-FM	PSNR	MPM
Proposed	91.00±1.67	91.09	93.67	19.34	0.32
Proposed (upper bound)	91.78±1.54	91.82	95.08	19.80	0.20
BE [9]	87.10±4.99	87.53	88.77	18.16	1.04
LMM [10]	85.49±4.63	85.73	92.55	17.83	0.42
Ms Gb Sauvola [1]	85.22±5.49	85.89	90.32	17.62	0.68
Sauvola MS_{kx} [40]	80.03±9.26	82.36	87.07	16.35	3.41
AdOstu [3]	86.01±4.81	86.25	91.63	18.04	**0.20**
PC [19]	88.52±2.40	88.69	90.37	18.08	0.63
Lelore [41]	-	**91.78**	94.43	19.67	1.33
LMM+ [2]	**92.03**	-	94.85	**20.12**	0.25
1^{st} top rank of contest	-	91.50	93.58	19.78	0.49
2^{nd} top rank of contest	-	89.70	**95.15**	19.15	0.28
Best results of contest	-	91.78	95.15	19.78	0.23

TABLE III: Comparison Of The Performance Of The Proposed Method And The Others Against Dibco'11 Dataset

Algorithm	FM±std	FM*	PSNR	MPM	DRD
Proposed	**91.42±2.99**	**91.56**	**18.68**	**0.91**	**2.74**
Proposed (upper bound)	92.57±2.34	92.62	19.29	0.55	2.28
BE [9]	81.67±13.48	83.32	15.59	11.34	11.23
LMM [10]	85.56±6.16	86.23	16.75	5.38	5.02
Ms Gb Sauvola [1]	84.15±9.13	85.50	16.32	10.25	7.00
Sauvola Ms_{kx} [40]	79.70±12.69	81.78	14.91	20.32	11.67
AdOstu [3]	86.12±4.85	86.58	16.88	2.58	4.36
PC [19]	87.74±5.49	88.18	17.02	1.91	4.59
LMM+ [2]	87.7	-	17.56	5.17	4.48
Gatos et. al [5]	84.3	-	16.3	6.39	6.08
Howe (static) [15]	89.2	-	18.2	9.05	5.76
1^{st} rank of contest [41]	80.86±29.11	86.19	16.13	64.36	104.47
Best results of contest	88.72±7.28	89.42	17.84	8.61	5.36

C. Enhancement of Other Binarization Methods

Preprocessing and main binarization in the proposed method are used as a mask to cross out false positive pixels on the output of other binarization methods, which resulted in an outstanding level of improvement. This mask has a high recall value with an acceptable precision value. Table VIII shows the improvement we achieved over other binarization methods using the proposed mask. Compared with previous works [12]–[14], which were aimed at modifying other binarization methods, our proposed method shows even more improvement. For example, in [14], the improved F-Measure values of Otsu's method for DIBCO'09, H-DIBCO'10, and DIBCO'11 are 81.98, 87.13, and 83.55 respectively. Our improved results are 89.82, 86.49, and 88.91 respectively.

D. Time Complexity

In this section, we evaluate the run time of our proposed method, performing our experiments on a Core i7 3.4 GHz CPU with 8 GB of RAM. The algorithm is implemented in MATLAB 2012a running on Windows 7. It takes 2.04 seconds to operate it on a 0.3 megapixel image, and 20.28 seconds to produce output for a 3 megapixels image. It is worth mentioning that the proposed algorithm would run faster and would require much less memory if the phase congruency features are calculated using the alternative monogenic filters of [43].

TABLE IV: F-Measure Improvement To State-Of-The-Artmethods Using Our Proposed Mask Image

F-M / Improved F-M	DIBCO'09	H-DIBCO'10	DIBCO'11	H-DIBCO'12
Otsu [56]	78.60 / 89.82	85.43 / 86.49	82.10 / 88.91	75.07 / 87.65
Niblack [39]	**52.30 / 89.80**	***45.86 / 89.32***	**44.69 / 89.72**	**45.62 / 88.59**
Grid based Sauvola [1]	88.17 / 90.75	84.65 / 85.05	84.46 / 88.95	85.60 / 86.34
Multi-scale Grid based Sauvola [1]	89.26 / 91.34	85.22 / 85.67	84.15 / 89.04	87.54 / 88.33
ESBK [3]	90.06 / 91.16	82.95 / 83.03	87.92 / 88.94	*86.00 / 88.94*
Su's method [10]	91.06 / 91.33	85.49 / 85.61	85.56 / 87.17	N/A
Lu's method [9]	*91.13 / 92.31*	87.10 / 87.92	*87.66 / 90.40*	N/A

VI. CONCLUSION

In this paper, we have introduced an image binarization method that uses the phase information of the input image, and robust phase-based features extracted from that image are used to build a model for the binarization of ancient manuscripts. Phase-preserving denoising followed by morphological operations are used to preprocess the input image. Then, two phase congruency features, the maximum moment of phase congruency covariance and the locally weighted mean phase angle, are used to perform the main binarization. For post-processing, we have proposed a few steps to filter various types of degradation, in particular, a median filter has been used to reject noise, unwanted lines, and interfering patterns. Because some binarization steps work with individual objects instead of pixels, a Gaussian filter was used to further separate foreground from background objects, and to improve the final binary output. The method has been tested on various datasets covering numerous types of degradation: DIBCO'09, H-DIBCO'10, DIBCO'11, H-DIBCO'12, PHIBD'12 and BICKLEY DIARY. Our experimental results demonstrate its promising performance, and also that of the postprocessing method proposed to improve other binarization algorithms.

VII. REFERENCES

[1] R. F. Moghaddam and M. Cheriet, "A multi-scale framework for adaptive binarization of degraded document images," Pattern Recognit., vol. 43, no. 6, pp. 2186–2198, 2010. Recognit., vol. 45, no. 6, pp. 2419–2431, 2012.

[2] J. Sauvola and M. Pietikinen, "Adaptive document image binarization," Pattern Recognit., vol. 33, no. 2, pp. 225–236, 2000.

[3] B. Gatos, I. Pratikakis, and S. Perantonis, "Adaptive degraded document image binarization," Pattern Recognit., vol. 39, no. 3, pp. 317–327, 2006.

[4] R. Hedjam, R. F. Moghaddam, and M. Cheriet, "A spatially adaptive statistical method for the binarization of historical manuscripts and degraded document images," Pattern Recognit., vol. 44, no. 9, pp. 2184–2196, 2011.

[5] S. Lu, B. Su, and C. Tan, "Document image binarization using background estimation and stroke edges," Int. J. Document Anal. Recognit., vol. 13, no. 4, pp. 303–314, 2010.

[6] B. Su, S. Lu, and C. Tan, "Binarization of historical document images using the local maximum and minimum," in Proc. 9th IAPR Int. Workshop DAS, 2010, pp. 159–166.

[7] B. Gatos, I. Pratikakis, and S. Perantonis, "Improved document image binarization by using a combination of multiple binarization techniques and adapted edge information," in Proc. 19th ICPR, Dec. 2008, pp. 1–4.

[8] B. Su, S. Lu, and C. L. Tan, "A self-training learning document binarization framework," in Proc. 20th ICPR, Aug. 2010, pp. 3187–3190.

[9] B. Su, S. Lu, and C. L. Tan, "Combination of document image binarization techniques," in Proc. ICDAR, Sep. 2011, pp. 22–26.

[10] B. Su, S. Lu, and C. L. Tan, "A learning framework for degraded document image binarization using Markov random field," in Proc. 21st ICPR, Nov. 2012, pp. 3200–3203.

[11] N. Howe, "Document binarization with automatic parameter tuning," Int. J. Document Anal. Recognit., vol. 16, no. 3, pp. 247–258, 2013.

[12] M. Cheriet, R. F. Moghaddam, and R. Hedjam, "A learning framework for the optimization and automation of document binarization methods," Comput. Vis. Image Understanding, vol. 117, no. 3, pp. 269–280, 2013.

[13] N. Howe, "Document image binarization using Markov field model," in Proc. ICDAR, 2011, pp. 6–10.